α-Al_2O_3 DIFFUSION BARRIERS TO ELIMINATE THE RADIOXENON MEMORY EFFECT IN PHOSWICH DETECTORS

W. K. Warburton, Stephen J. Asztalos, and Wolfgang Hennig

XIA LLC

Sponsored by the National Nuclear Security Administration

Award No. DE-NA000486
Proposal BAA10-73

ABSTRACT

Well designed detectors, including such examples as ARSA, SAUNA, and XIA's "PhosWatch", can readily achieve the state of the art radioxenon detection limits required for nuclear explosion monitoring. They are also reliable, robust detectors that do not require cryogenic cooling for operation. All three employ the principle of beta-gamma coincidence detection to reduce background counting rates, using a BC404 plastic scintillator to detect the betas and a CsI(Tl) or NaI scintillator to detect the gamma-rays. As a consequence of this commonality of design, all three also display a "memory effect" arising from the diffusion of Xe into BC404. Thus, when one sample is pumped out of the detector, a fraction remains behind, embedded in the BC404, where it artificially raises the signal counting rate for the next sample. While this is not a fatal flaw in phoswich detectors, developing a method to eliminate the memory effect would significantly enhance their utility.

In this work we proposed to develop thin, amorphous Al_2O_3 films to act as diffusion barriers on the BC404 surfaces exposed to radioxenon. The amorphous property is critical, since it eliminates the high diffusivity grain boundaries that occur with high densities in thin crystalline films, and Al was selected since it is known to naturally form high density amorphous films in thin layers. While we initially proposed to grow the films by depositing Al in a low pressure oxygen environment, our subsequent research revealed that ALD (atomic layer deposition) was a superior alternative, particularly because it could deposit uniform layers on arbitrarily curved surfaces (e.g. the spherical interior of the PhosWatch's BC404 detector). We therefore established a collaboration with Prof. Steven George and his group at the University of Colorado, Boulder, who are internationally known for their work on ALD and ALD deposited Al_2O_3 films in particular. Prof. George's group has, for example, developed methods to grow Al_2O_3 films that are impenetrable by H_20, a molecule that is significantly smaller in diameter than Xe.

Our experimental approach is therefore as follows. We have designed and built a "doser" that uses an old PhosWatch detector to deliver a calibrated dose to thin cylindrical BC404 samples. We have also built a custom counting jig to reproducibly count the BC404 samples in a phoswich geometry using a 2" CsI(Tl) crystal. Prof. George's group has created one set of BC404 samples coated with 4 thicknesses of Al_2O_3 at one temperature and another set of the same thickness coated at 3 different temperatures so that we can explore the parameters that create the highest quality films. We are currently developing our dosing and counting techniques using radon, which is readily available and also shows the memory effect, and then will repeat our measurements with radioxenon, which is harder to obtain and handle.

Initial results with radon show a rapid initial decay in the memory effect (time constant about 1 hour) followed by a slower decay rate typical of the normal radon half life. Our present interpretation is that the shorter half life reflects diffusion of radon out of the test samples, while the slower component is a combination of radon remaining in the sample and detector contamination. The latter is most probably from exposure to atmospheric radon, since we also see it in undosed background samples. This suggests that the background effect might be substantially reduced by changing the standard measurement protocol to replace the present eight hour background measurement with an eight hour continuous pumpout.

OBJECTIVES

XIA, under support from the DOE's SBIR program, has developed a "PhosWatch" phoswich radioxenon detector to potentially support CTBTO verification operations [Hennig, 2009]. This detector employs a nearly spherical Xe sample shell of BC-404, 1-2 mm thick, embedded in a 3" diameter cylinder of CsI(Tl) that is 3" high and coupled to a single PMT. The PMT is coupled to a digital spectrometer that uses pulse shape analysis to identify radioxenon decays. Specifically, most radioxenon decays emit either a beta particle or a conversion electron in coincidence with either a K x-ray or a relatively low energy gamma-ray. When such a decay occurs in the BC-404 sample shell, the electron is captured with nearly 100% efficiency in the BC-404, while the photon is captured with a high probability in the CsI(Tl) crystal. The resulting PMT pulse shape then has a characteristic shape, with a sharp spike of light from the BC-404 (which has a decay time of order 10 ns) followed by a much slower light emission from the CsI(Tl) (decay times in the μsec range). This "pulse shape coincidence" technique has a very high rejection ratio against various types of background radiation (gamma-rays, Compton scattering, alpha particles, etc.). As the energies of both the electron and photon can be individually extracted, the various radioxenon isotopes can be identified to some degree. PhosWatch performance has been shown to be comparable to both SAUNA and ARSA detectors, but it is less complex, cheaper, and much simpler to operate and keep calibrated under remote service conditions.

Like the SAUNA [Ringbom, 2003] and ARSA [McIntyre, 2001] detectors, however, the PhosWatch suffers from the "radioxenon memory effect" [Seifert – 2005], which is understood to arise from the diffusion of radioxenon into the BC-404 plastic (polyvinyltoluene) during counting. As a results, when samples are changed (by pumping out one radioxenon charge and admitting another), some fraction of the previous sample remains, buried within the walls of the BC-404 sample cell. This residual "old" radioxenon can then distort the collected spectrum that is supposed to represent the "new" radioxenon sample, particularly if the first sample was much more active than the second. Thus, the detector "remembers" previous samples because of the diffusion process. While, at some level, it is possible in principle to correct each sample measurement, based on the results of previous sample measurements, doing so can greatly degrade the statistical accuracy of measurements upon which issues of national and international security ride. If means can be found to eliminate the memory effect, they would be far preferable.

In this effort, our proposed approach to eliminating the memory effect is by coating the inside surface of the BC-404 sample shell with a "vapor barrier" of amorphous aluminum oxide (α-Al_2O_3) that would prevent the radioxenon from reaching the BC-404 and thus from diffusing into it. Al_2O_3 was chosen both because it is a dense inorganic material (and thus should not have large internal free volumes to allow the diffusion of Xe atoms) and because it is transparent in thin sections and so will not interfere with light collection within the PhosWatch geometry. It is also chemically very inert, which is desirable for the long term stability of the treatment. Finally, the amorphous form was chosen both because it is known that it is very hard to produce continuous crystalline films in thin sections and, even when achieved, the grain boundaries between the crystallites are both fast diffusion channels and, being physically separated by distances comparable to the film's thickness, are also extremely numerous.

Our proposed effort therefore contained the following major components:

- Develop a method to deposit α-Al_2O_3 on both test samples of BC-404 and the Phoswatch's cell, a hollow spherical shell;
- Develop a method to reproducibly expose coated BC-404 samples to radioxenon and measure their memory effect;
- Use this method to study the memory effect as a function of film growth and thickness parameters;
- Develop an optimized film growth process:
- Apply this film to a BC-404 shell in a PhosWatch detector and demonstrate the resulting reduction in memory effect.

RESEARCH ACCOMPLISHED

GROWTH METHOD for α-Al_2O_3

Since it is known that thin α-Al_2O_3 spontaneously grows on Al when exposed to oxygen, our initial concept was to grow α-Al_2O_3 by slowly evaporating Al onto BC-404 in the presence of a low background pressure of oxygen. We proposed to first grow such films on BC-404 flats and test them for their ability to block radon and Xe diffusion, thereby developing a acceptable growth technology, and then to move on to transfer the method to the deeply curved BC-404 sample cell halves.

We began our research with an online search made using Elsevier's SCOPUS service, which discovered essentially no new references, beyond those noted in our proposal, relating to the growth of α-Al_2O_3 by the direct oxidation of an Al film during its deposition. However we did discover a different deposition technology with which we were previously unacquainted – Atomic Layer Deposition (ALD) – which has been developed over the last 10-15 years, primarily by a group at the University of Colorado, Boulder, under the direction of Professor Stephen George [George, 2010]. This technique works by using self-limiting surface reactions to build up materials one atomic layer at a time. Taking α-Al_2O_3 for example: first the substrate is exposed to gaseous tri-methyl-aluminum ($Al(CH_3)_3$), which binds to produce a single monolayer on the surface and then does not react further. The $Al(CH_3)_3$ is then pumped away and the surface is exposed to water vapor, which reacts to form a single layer of α-Al_2O_3 and, when the $Al(CH_3)_3$ has all been reacted, stops. The water vapor is then pumped away and the cycle repeated to build up a thick a layer of α-Al_2O_3 as desired.

In fact, α-Al_2O_3 has been much studied by Prof. George's group for many of the same reasons we selected it for this study, particularly including its inertness and its ability to form defect free chemical or vapor barriers. The group has an ongoing interest in coating plastics with α-Al_2O_3 to form water vapor barriers (to create products as diverse as food protection wraps and fuel cell membranes). Layer defects densities as low as $20/cm^2$ have been routinely produced, with these primarily resulting from dust particles on the surfaces and not from any inherent limitation in the deposition technique itself. Because the deposition reactants are gases, there are essentially no limitations on substrate topology and good films have been formed in etched Si structures with aspect ratios of over 2000-to-1.

The work on α-Al_2O_3 grown on plastics further showed that the process works with almost any plastic and that diffusion of the reactant $Al(CH_3)_3$ into the plastic surface not only formed a robust bond between the plastic substrate and the α-Al_2O_3 film, but also enhanced the properties of the α-Al_2O_3 as a diffusion barrier by filling and “clogging” the largest diffusion pathways at the surface [Wilson, 2005]. α-Al_2O_3 film growth was studied as a function of temperature (as some plastics cannot withstand high deposition temperatures) and it was found that satisfactory films could be grown down to 30 °C, but that growth times became quite long and the films were not quite as dense. Optimum growth occurred at about 120 °C.

Since Prof. George's group was attaining essentially theoretical α-Al_2O_3 density (i.e. one could not expect to grow denser films by other methods), had experience in depositing on plastics, and has shown that the method would work on deeply curved substrates (one of the most problematical issues of the present proposal was the issue of how to deposit Al uniformly on the inside of a sphere with a 1/2” radius) we contacted Prof. George and proposed a collaboration, which Prof. George agreed to. A visit to his laboratory was hosted by his senior graduate student, Mr. Jacob Bertrand. Mr. Bertrand is the laboratory's local expert on Al2O3 film growth and, for his thesis work, is perfecting it as a water vapor barrier. In discussions, Mr. Bertrand pointed out to the PI that water molecules are actually smaller than the Xe atoms whose diffusion we seek to block and that a strongly water resistant film should also be excellent for stopping Xe. In the course of these discussions, Mr. Bertrand agreed to make some test BC-404

Table 1: Initial deposition schedule

Temperature (°C)	Thickness (nm)	Quantity
75	7	4
100	7	4
125	2	4
125	5	4
125	7	4
125	10	4
150	7	4

Table 2: Revised deposition schedule

Temperature (°C)	Thickness (nm)	Quantity
75	7	4
85	7	4
100	2	4
100	5	4
100	7	4
100	10	4
125	Bubbled	4

coatings for us, on either planar or spherical shell samples, so that we could evaluate the film's ability to block the diffusion of an atomic species that was new to their experience.

In order to decide upon deposition temperatures, we contacted St. Gobain about its temperature characteristics. While BC-404 has a listed softening point of 70 ºC, the St. Gobain representative claimed that it could go much higher without deformation over short time frames. Since Mr. Bertrand's results point to improving film quality as they move from deposition temperatures of 30 ºC to 120 ºC, after some discussions, we decided upon the initial deposition program shown in Table 1, where the sequence at the preferred 125 °C deposition temperature would investigate the effectiveness of different film thicknesses in preventing Xe diffusion, while the sequence of 4 temperatures at 7 nm thickness would investigate the influence of deposition temperature on film quality, vis as vis preventing Xe penetration. This selection of temperatures was based on two criteria: first that the deposition proceeds much more rapidly at higher temperatures and typically gives better film quality as well; and, second, that, while 70 °C is listed at the softening point of BC-404, it is cast at much higher temperatures.

In practice, Mr. Bertrand's first attempt to coat samples at 125 °C destroyed the samples, which not only flowed, but also showed internal bubbling. Based on Dr. Warburton's conjecture that this behavior resulted from water absorbed by the BC-404 vaporizing and expanding within the softened plastic at 125 °C, Mr. Bertrand next tried depositing a 2 nm coating on samples at 100 °C after first baking them at 70 °C overnight to outgas the water. These samples did not bubble, although their bottom surface roughened a bit from contact with the reactor surface. Mr. Bertrand solved this problem by placing all subsequent samples onto polished Si wafers for the deposition procedure. He has now produced a set of samples according to the revised deposition schedule shown in Table 2 and returned them to XIA for testing.

The Figures show some details of this work. Figure 1 shows a picture of the ALD reactor in Prof. George's laboratory. Figure 2 shows one of the first 125 °C samples, displaying the bubbling noted above. Figure 3 shows one of the 100 °C samples prepared using both the Si wafer support and the 70 °C overnight bakeout. As may be seen, the optical quality is very good. Mr. Bertrand has now produced all of the samples in Table 2 and they are awaiting testing in our laboratory.

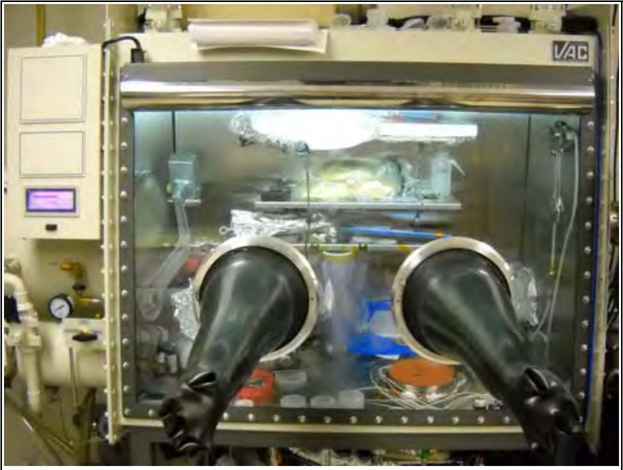

Figure 1: ALD reactor in Prof. George's Laboratory.

Figure 2: Bubbled 125 °C BC-404 sample.

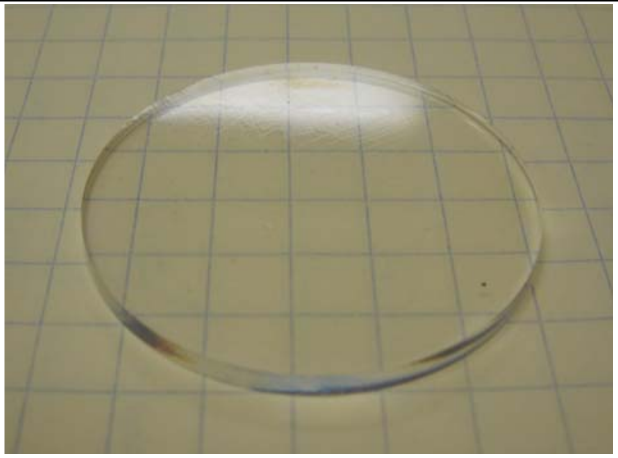

Figure 3: Improved 100 °C process BC-404 sample.

EXPERIMENTAL EQUIPMENT for MEASURING the MEMORY EFFECT

In preparation for the radioxenon measurements we created two pieces of equipment. The first was a “doser” system to expose our samples to a reproducible dose of either radon or radioxenon. The second was a “memory effect test jig” to measure the dosed samples and determine their uptake of gas, if any.

THE DOSER SYSTEM

We have investigated the procurement of radioxenon and have found two choices. The first is to have it made for us (pending a lengthy approval process which just completed in late June) in a reactor at the McClellan Nuclear Research Center at University of California, Davis. The other is to subcontract with Prof. Steven Biegalski at the University of Texas. (Obtaining radioxenon from medical isotope suppliers has not proven feasible at this point due to licensing requirements and their unwillingness to provide exempt amounts.) In either case, the amount of time available for measurements after each batch of radioxenon is produced will be relatively short, given even its longest half life. Therefore we began our work with radon, which also shows the memory effect in BC-404, to perfect our measurement techniques so that, when we finally get to work with radioxenon, all our methods will be reproducible, reliable, and well rehearsed.

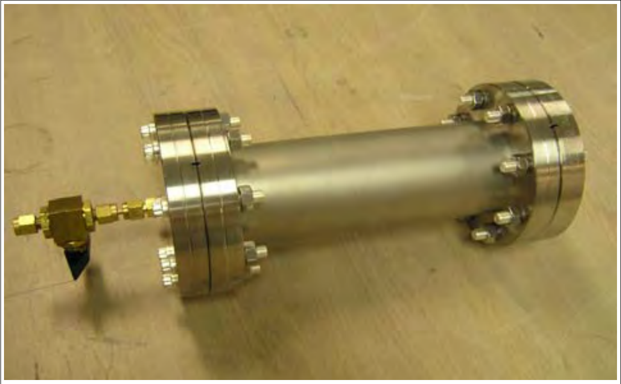

Figure 4: 1 liter Rn equilibration volume.

We are producing the Rn from a NIST calibrated source that XIA already owns. This source emits Rn at about 5,000 Rn atoms/sec. We enclosed it in an air filled volume of about 1 liter (Fig. 4) and let the concentration of Rn in the volume approach equilibrium (5,000 Bq/liter). An equilibration curve for this source, Fig. 5 shows that this process takes about 23 days. Then, each time we wish to test a BC-404 sample, we draw off about 10 cc of the Rn/air mixture into a dosing chamber (Fig. 6) containing the BC-404 sample, thereby exposing it to a 50 Bq Rn source. After an exposure period of a few hours, the Rn is pumped away and the BC-404 sample removed from the doser and inserted into the memory effect test jig for measurement. Within the doser, which is made from a pair of modified ConFlat flanges, the face of the BC-404 facing the Rn is sealed with an O-ring. To assure that any Rn that might diffuse through the O-ring cannot possibly reach untreated BC-404 surfaces we have taken two precautions. 1) The doser is designed so that N_2 gas can be injected the space outside the O-ring to flush away any such diffusing Rn; 2) the back of the doser is cut away so that no Rn can accumulate next to the sample's back face, it's other large surface area.

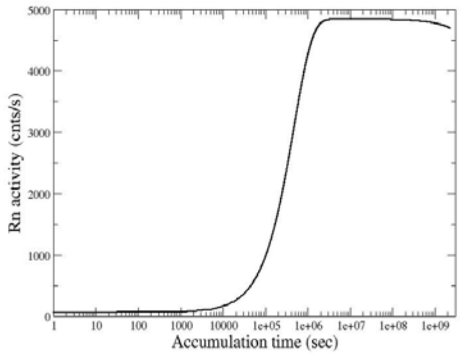

Figure 5: Rn equilibration in a fixed volume.

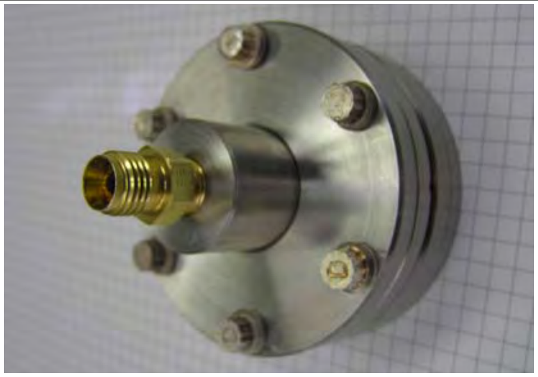

Figure 6: Chamber for dosing BC-404 with Rn.

THE MEMORY EFFECT TEST JIG:

The function of the memory effect test jig is to reliably recreate a planar beta-gamma phoswich detector by pressing a sample disk of BC-404 against a canned CsI(Tl) scintillator that, in turn, is coupled to a PMT with the entire assembly contained within a light tight container. Figure 7 shows a SolidWorks exploded view of our design.

Starting from the right, we have a PMT with its blue base and divider network cover, followed by the CsI(Tl) crystal, which

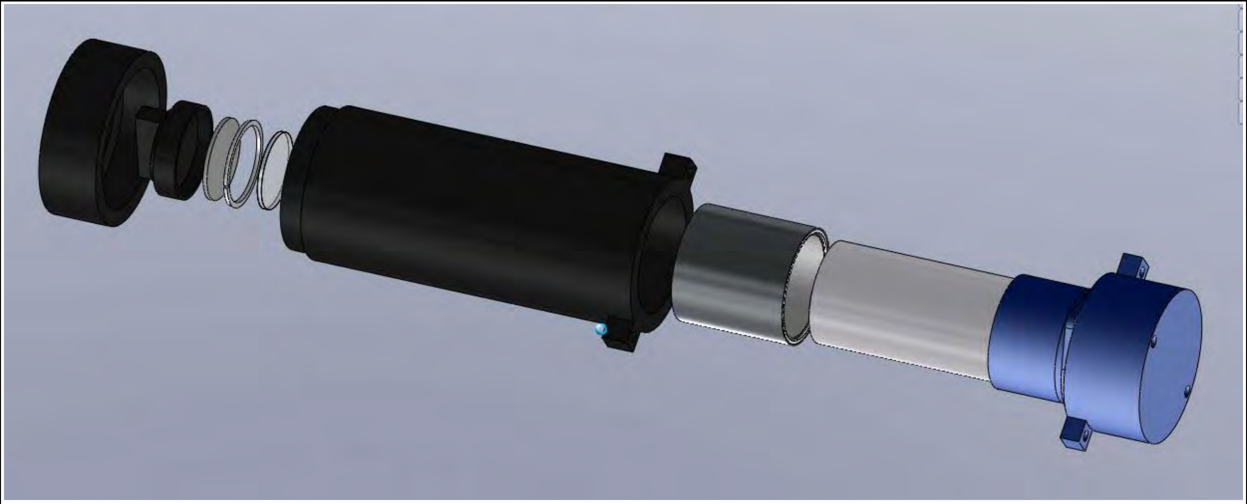

Figure 7: Exploded view of memory effect test jig.

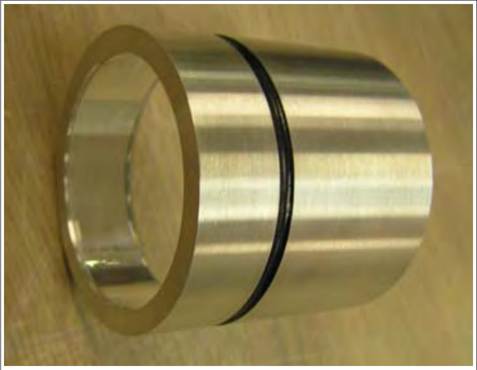

Figure 8: CsI(Tl) crystal.

Figure 9: Memory effect test jig parts, disassembled.

Figure 10: Sample mounting parts.

is in an Al can with a standard glass window towards the PMT and an 0.4 mm sapphire window toward the BC-404 sample. Sapphire was chosen for its strength and low x-ray absorption coefficient. Next is a black plastic shroud with an internal shoulder to provide a stop for the CsI(Tl) crystal, and on its left end, a thread to mate to a cap. Next comes the BC-404 sample, a Teflon collet, a black plastic collet clamp, and the cap. Images of the completed jig are shown in Figures 8 – 10. Figure 8 shows the completed CsI(Tl) crystal, viewed from its sapphire window end. Figure 9 shows the complete, disassembled test jig. The design of the BC-404 crystal holder is particularly interesting, as it is intended to allow the crystals to be readily exchanged while maintaining a highly reproducible light yield into the PMT. Fig. 10. shows a closeup of these parts. In the lower right is a Teflon “collet” that clamps the BC-404 tightly around its rim when laterally compressed. Its outside edge is tapered, as is the inside edge of the black collet holder, so that the clamping action takes place as the holder is pressed down onto the collet.

The white disk is a circle of Tyvek printing paper that has at least 98.5% reflectivity. The full assembly is a stack comprising the BC-404 crystal, the Tyvek circle, a circle of thin sponge, the collet, and the collet holder. This stack is placed on the face of the CsI(Tl) crystal and clamped to it using the threaded collet holder clamp. In practice there will also be thin layers of optical coupling grease between the BC-404 and the CsI(Tl) crystal's sapphire window and between the PMT and its glass window. The BC-404 will thus always be identically aligned with respect to the CsI(Tl) crystal and also have reproducible white material both on its flat face and edges.

RESULTS from MEASUREMENTS with RADON

A new, undosed sample NC1 of BC-404 was placed into the test jig and measured to examine background rates. The test jig was placed in XIA's counting cave (2” of Pb and 0.5” of Cu) and counted using a XIA Pixie-4 spectrometer running a variant of the code that we developed for our PhosWatch detectors. The resulting 2-D β–γ decay spectrum that plots CsI(Tl) response (y axis) versus BC-404 response (x-axis) is shown in Figure 11. The vast majority of counts are CsI(Tl) only counts (on the left axis) that spill a little bit into the coincidence area due to statistical fluctuations in the counts in the area where the CsI(Tl) and BC-404 pulse shapes overlap. The average background rate is about 4 cps. The same sample was then dosed for 4 hours in the doser described above and replaced into the test jig for counting. Figure 12 shows the result for 4 hours of counting.

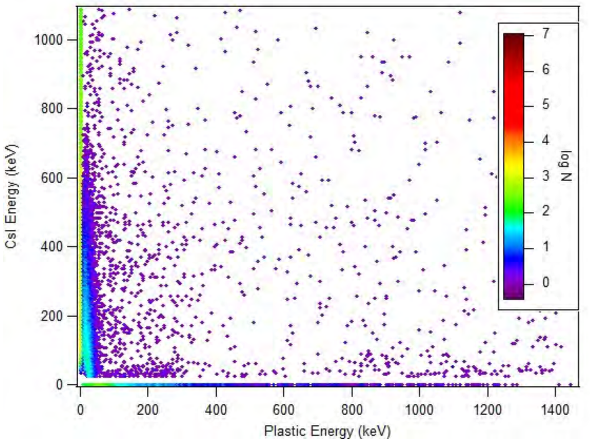

Figure 11: Background spectrum, no Rn dose.

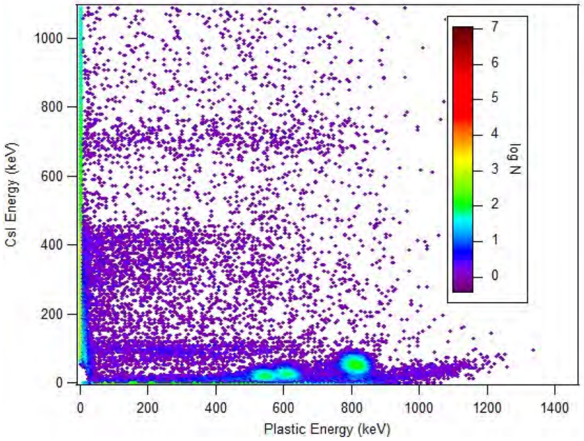

Figure 12: Spectrum after 4 hour Rn dose.

This Rn spectrum has the usual characteristic features. 1) Three strong alpha particle peaks near 600 and 800 keV on the BC-404 axis. These are, respectively, 222-Rn at 5,489 keV, 218-Po at 6,002 keV, and 214-Po at 7,687 keV. Because of the quenching that accompanies the high charge densities produced in the scintillator during alpha particle absorption, the energy scale for the alpha particles is much smaller (by a factor of about 10) than for the electrons used to calibrate the BC-404 energy scale. The quenching also produces a slightly different pulse shape from electron interactions, causing the alpha events fall on a slightly sloped line, compared to electron events that fall on the bottom axis. 2) Coincidence lines from beta decays at energies near 100 keV, 300 keV, 400 keV, and 700 keV. Because this detector has not yet been carefully calibrated, the y axis reads about 15% high. The identities of these lines are as follows. At 100 nominal keV, we have the three 214-Pb K x-ray lines (75 keV, 6.5%; 77 keV, 11.0%, & 87.2 keV, 3.9%) in coincidence with a beta particle and/or a conversion electron over a range of energies up to about 600 keV. Similarly its three major gamma-rays (242 keV, 7.4%; 295 keV, 19.3%; and 352 keV, 37.6%) appear at energies between 300 to 400 keV. The final major coincidence line at about 700 keV is a 214-Bi gamma-ray (609 keV, 46.1%). The next gamma-ray line at 882 keV (768 keV, 4.9%) is too weak to be seen at this level of statistics. The 214-Bi lines are in coincidence with a beta particle of up to about 1,200 keV and we see that the line at 700 keV is indeed about twice as long as the 214-Pb lines below it. We thus see that the Rn spectrum is readily identifiable in a beta-gamma coincidence plot.

Using uncoated BC-404 samples, we next performed a series of experiments intended to develop a method for delivering a controlled Rn dose to the sample. In this process, we attached an early PhosWatch detector to our dosing system and, after evacuating the connecting line, opened the valve between the Rn source and the doser for a fixed time of 10 seconds. We then used the PhosWatch coincidence counting rate as a measure of the dosing rate being applied to the sample. The samples were exposed for 4 hours and then counted in the test jig for 4 hours. The difference between this count and the background count over all the beta-gamma coincidence region except the y axis was taken as a measure of the sample's memory effect. Unfortunately, we found neither reproducibility in the PhosWatch counting rates, trial to trial (up to factors of two) nor any correlation between the PhosWatch measured exposure and the sizes of the observed memory effects, which also varied by factors of two, but independently of the “dose” value.

Working to understand and eliminate these variations, we began a systematic study of our dosing system components. Issues uncovered to date include: 1) valves that leak into their internal volumes so that they “burp” air into the system when opened or closed, but don't leak when static. 2) Rapid loss of Rn from the test samples. 3) Non-reproducible backgrounds that show significant amounts of Rn. We will fix the first problem by rebuilding the dosing system with a higher grade of vacuum valve. The other two issues deserve further comment.

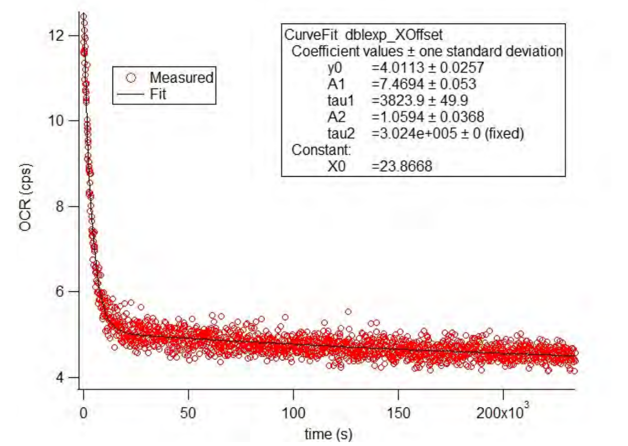

Figure 13: Output count rate from dosed NC-5 sample.

RAPID RADON LOSS from BC-404

Figure 13 shows the test jig raw output counting rate as a function of time in a experiment where the sample NC5 was dosed for 4 hours, removed from the doser, allowed to “outgas” for 5 minutes, installed in the test jig and counted for almost 67 hours (2.6 days). The curve shows two clear classes of behavior. First, the count rate, which is initially almost 13 cps, drops to close to 5 cps with an exponential time constant of 1.06 ± 0.01 hours. After that the rate is well fitted by an exponential decay term with amplitude 1.12 and the 3.825 day half life of 222-Rn plus a fixed background rate of 3.93 cps. Two slightly different scenarios would produce this result. In both, the rapid term represents rapid loss of 222-Rn from the BC-404 sample by diffusion into the (effective) vacuum of the test jig. The remaining, slowly decaying 222-Rn would then come from either residual 222-Rn that was somehow trapped in the BC-404 or else from 222-Rn that contaminated the test jig and is therefore a “background” term. To evaluate these two possibilities we performed two additional experiments.

RADON BACKGROUND COUNT TESTS

In the first experiment, we disassembled the test jig and baked it in an open air oven for 24 hours at 40 °C. We also dosed a sample NC2 for 6 hours that had last seen Rn 28 days previously (i.e. should be at background) and also baked it for 10 hours, also at 40 °C. We then placed it into the test jig and counted it. Its spectrum is shown in Figure 14 and is clearly a 222-Rn spectrum whose counting rate is shown in Figure 15, where we see that it fell from about 5.8 cps to 5.1 cps over 4 hours. An exponential fit shows a very small initial fast decay of amplitude 0.78 and a decay time of 0.98 ± 0.22 hours, which is statistically the same as before. The total counting time is not long enough

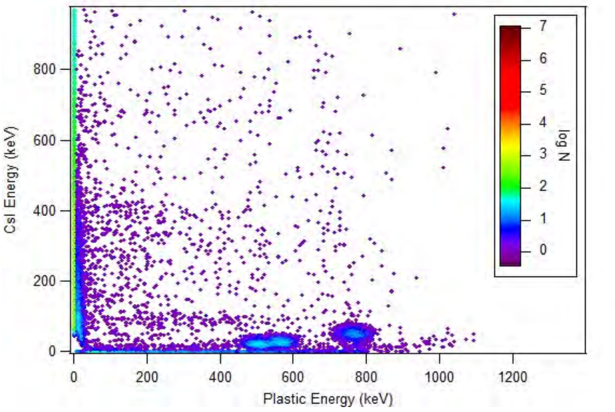

Figure 14: NC-2 Spectrum after 8 hour Rn dose and 10 hour bake at 40 °C.

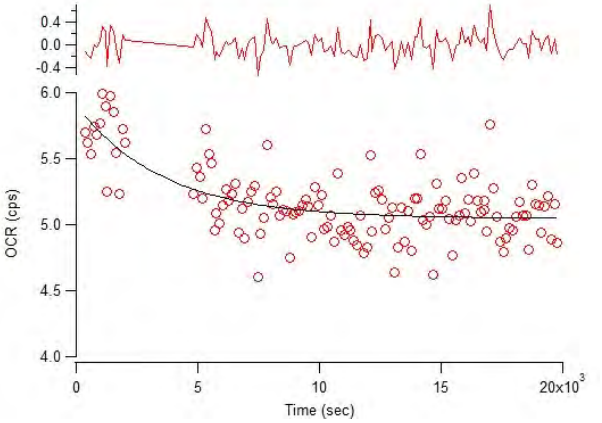

Figure 15: NC-2 OCR versus count time.

to look for the decay of the remaining 222-Rn, which would (presumably) finally reduce the count rate to the background value of about 4..

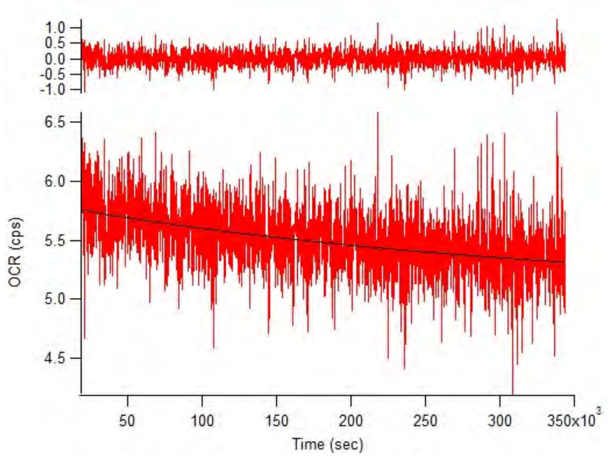

Figure 16: NC-1 OCR versus count time.

In the second experiment, we then removed NC2 from the test jig and replaced it directly with sample NC1, which had not been dosed with radon for over 30 days, and started counting immediately. This sample counted for over three days and also shows a 222-Rn spectrum. The OCR, shown in Figure 16, has a single exponential decay term matching 222-Rn's half life and an amplitude of 0.70 cps. An expansion of the first 4 hours of counting shows that, if there is a fast term it must be smaller than the 0.5 cps noise amplitude. The initial counting rate here is about 5.75 cps, almost 1 cps higher than the last rate from the previous sample, although no new radon was intentionally added to the system. This suggests that the decaying 222-radon background we saw in the two previous experiments was not due to either radon trapped in the BC-404 sample or test fixture contamination since both of these terms would have decreased between the second and third experiments. Based on these results, we now believe that the most likely source of 222-Ra is atmospheric radon that contaminates the sample and inner test jig surfaces each time the sample is changed. Because this amount would vary both with the time it took to make the sample change and the amount of radon in the air, which is known to fluctuate widely, we would not expect the resultant background count rate to be particularly reproducible.

ANALYSIS

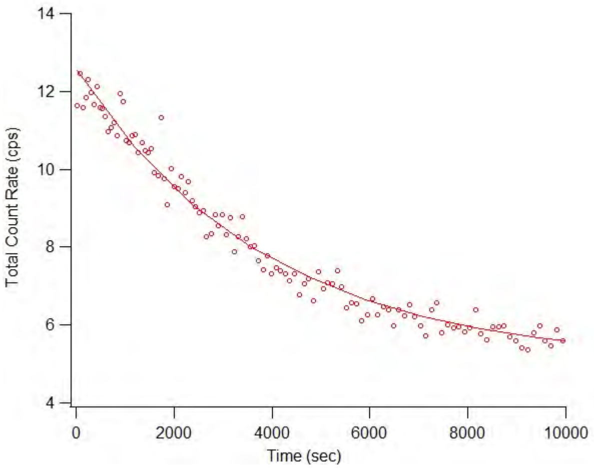

Figure 17: NC-5 OCR (Figure 13) at short count times.

At this stage we believe that two factors have conspired to generate irreproducible results: the initial fast decay component and a variable dose of “atmospheric” radon added to each measurement. The latter can easily add from 1 to 3 cps, which is up to a 20% variance in an initial radon counting rate of 10 cps. Secondly, the rapid decline means that modest changes in time to start counting after the dose and introduce large variation in the amount of radon left in the sample. Further, because the initial slope of the decay curve is steep, it is hard to get an accurate fit to its initial value. Figure 17 shows the short time dependence of sample NC-5 (Figure 13). This suggests that further radon experiments should be carried out in a glove box filled with nitrogen or argon, both of which are available to us. Further, to avoid the possibility of contaminating the test jig with either radon or radioxenon with gas diffusing out of the sample and into the plastic parts of the test jig, either the design should be changed so that sealed samples can be dosed, preferably directly within the test jig, or that the test jig should be remade of materials that do not absorb radon or radioxenon, or both.

CONCLUSIONS AND RECOMMENDATIONS

In summary, we have performed a variety of experiments intended to prepare for precise radioxenon memory effect measurements. In the process we have become acutely aware of the difficulties inherent in working with a gas that diffuses readily into plastics and is also present at significant levels in the atmosphere. Our major discovery to date is that, at approximately 25 °C, radon appears to diffuse out of BC-404 with a time constant of about 1 hour. If verified for radon and subsequently shown to be true for xenon as well, which is likely since Xe is a smaller atom that Rn and hence diffuses even more rapidly, then this result suggests a second approach to overcoming the memory effect, namely extended pumping.

In present standard practice, the radioxenon is removed from beta-gamma coincidence detectors such as the PhosWatch or SAUNA detectors using a protocol in which the Xe cell is evacuated and flushed with an inert gas a small number of times over a short period of approximately 10 minutes. Then another (typically) 8 hour count is started again to measure the background resulting from any residual radioxenon trapped in the BC-404 cell walls. However the cell is typically sealed during this count, so that radioxenon diffusing out of the cell walls remains trapped within the cell volume. Thus, while the amount of radioxenon initially trapped in the cell walls is indeed accurately measured, whether or not this accurately reflects the "memory effect" contribution to the next count depends upon whether or not the cell is evacuated a final time prior to the introduction of the next radioxenon sample. If it is evacuated, then a significant fraction of the measured activity (i.e. the gas that has diffused back into the volume) will be removed and the correction term for the next count will be accordingly in error.

Now if, instead, the cell were to be pumped for the same time as the background count, our measurements suggest that a large fraction of the gas in the wall should diffuse into the pumped volume and be removed from the system. If true, then a significant fraction of the memory effect could be reduced by a simple change in measurement protocol. In the most optimistic result, it could work well enough to avoid having to apply coatings to the BC-404 cells at all, which would be a major advantage, particularly for instruments already in the field. In any case, if a background count were taken simultaneously and fitted with an exponential decay, then the residual amount of radioxenon would be the best estimate of any remaining memory effect. In our future work we will therefore attempt to characterize this phenomenon carefully, particularly to study its dependence on both temperature (since diffusion is thermally activated) and longer dosing time (since desorption times should increase with increasing absorption times and deeper radioxenon penetrations into the BC-404 cell walls). In the present work the dosing time was 7 hours and the outgas time was 10 hours. It will be extremely interesting to see what fraction of a 24 hour dose can be removed with an 8 hour out-gassing period.

ACKNOWLEDGEMENT

We greatly appreciate the willingness of Dr. Stephen George and Mr. Jacob Bertrand at the University of Colorado, Boulder to collaborate with us and grow ALD α-Al_2O_3 films for this research. We hope to begin investigating their properties in the near future.

REFERENCES

George, S.M. (2010), Atomic Layer Deposition: An Overview, *Chem. Rev.* 110:113–131.

Hennig, W., W. K. Warburton, A. Fallu-Labruyere, K. Sabourov, M.W. Cooper, J. I. McIntyre, A. Gleyzer, M. Bean, E.P. Korpach, K. Ungar, W. Zhang, and P. Mekarski (2009), Development of phoswich detector system for radioxenon monitoring, *J. Radioanalytical & Nuclear Chemistry* 282: 681

McIntyre, J.I., Abel, K.H., Bowyer, T.W., Hayes, J.C., Heimbigner, T.R., Panisko, M.E., Reeder, P.L., and Thompson, R.C.(2001), Measurements of ambient radioxenon levels using the automated radioxenon sampler/analyzer (ARSA), *J. Radioanalytical & Nuclear Chemistry*, 248:629–635.

Ringbom, A., T. Larson, A. Axelson, K. Elmgren, and C. Johansson (2003), SAUNA—a system for automatic sampling, processing and analysis of radioactive xenon, *Nuclear Instruments and Methods in Physics Research* A 508: 542–553.

Seifert, C.E., J.I. McIntyre, K.C. Antolick, A.L. Carman, M.W. Cooper, J.C. Hayes, T.P. Heimbigner, C.W. Hubbard, K.E. Litke, M.D. Ripplinger & R. Suarez (2006), Mitigation of memory effects in beta scintillation cells for radioactive gas detection, in *Proceedings of the 27th Seismic Research Review: Ground-Based Nuclear Explosion Monitoring Technologies*, LA-UR-05-6507, Vol. 2, pp. 804–814.

Wilson, C.A., R.K. Grubbs, & S.M. George (2005), Nucleation and Growth during Al_2O_3 Atomic Layer Deposition on Polymers, *Chem. Mater*.17:5625–5634.